

CONF-961005--16

GA-A22427

**PRACTICAL BETA LIMIT IN ITER-SHAPED
DISCHARGES IN DIII-D AND ITS INCREASE
BY HIGHER COLLISIONALITY**

by

R.J. LA HAYE, J.D. CALLEN, M.S. CHU, S. DESHPANDE,
T.A. GIANAKON, C.C. HEGNA, S. JARDIN, L.L. LAO, J. MANICKAM,
D.A. MONTICELLO, A. PLETZER, A.H. REIMAN, O. SAUTER,
E.J. STRAIT, T.S. TAYLOR, A.D. TURNBULL, and H.R. WILSON

MASTER

DISTRIBUTION OF THIS DOCUMENT IS UNLIMITED

OCTOBER 1996



DISCLAIMER

**Portions of this document may be illegible
in electronic image products. Images are
produced from the best available original
document.**

DISCLAIMER

This report was prepared as an account of work sponsored by an agency of the United States Government. Neither the United States Government nor any agency thereof, nor any of their employees, makes any warranty, express or implied, or assumes any legal liability or responsibility for the accuracy, completeness, or usefulness of any information, apparatus, product, or process disclosed, or represents that its use would not infringe privately owned rights. Reference herein to any specific commercial product, process, or service by trade name, trademark, manufacturer, or otherwise, does not necessarily constitute or imply its endorsement, recommendation, or favoring by the United States Government or any agency thereof. The views and opinions of authors expressed herein do not necessarily state or reflect those of the United States Government or any agency thereof.

GA-A22427

PRACTICAL BETA LIMIT IN ITER-SHAPED DISCHARGES IN DIII-D AND ITS INCREASE BY HIGHER COLLISIONALITY

by

**R.J. LA HAYE, J.D. CALLEN,* M.S. CHU, S. DESHPANDE,†
T.A. GIANAKON,* C.C. HEGNA,* S. JARDIN,† L.L. LAO, J. MANICKAM,†
D.A. MONTICELLO,† A. PLETZER,‡ A.H. REIMAN,† O. SAUTER,‡
E.J. STRAIT, T.S. TAYLOR, A.D. TURNBULL, and H.R. WILSON^Δ**

This is a preprint of a paper to be presented at the Sixteenth IAEA International Conference on Plasma Physics and Controlled Nuclear Research, October 7-11, 1996, Montreal, Canada, and to be published in *The Proceedings*.

*University of Wisconsin, Madison, Wisconsin.

†Princeton Plasma Physics Laboratory, Princeton, New Jersey.

‡CRPP-EPFL, Lausanne, Switzerland.

^ΔUKAEA Fusion, Culham, Abingdon, United Kingdom.

Work supported by the U.S. Department of Energy
under Contract Nos. DE-AC03-89ER51114, DE-AC02-76CH03073,
and Grant No. DE-FG02-92ER54139, and in part by Swiss National
Science Foundation and U.K. Department of Trade and Industry
and EURATOM

**GA PROJECT 3466
OCTOBER 1996**



F1-CN-64/AP1-21

**PRACTICAL BETA LIMIT IN ITER-SHAPED DISCHARGES
IN DIII-D AND ITS INCREASE BY HIGHER COLLISIONALITY****ABSTRACT**

The maximum beta which can be sustained for a long pulse in ITER-shaped plasmas in DIII-D with $q_{95} \geq 3$, ELMs, and sawteeth is found to be limited by resistive tearing modes, particularly $m/n = 3/2$ and $2/1$. At low collisionality comparable to that which will occur in ITER, the beta limit is a factor of two below the usually expected $n = \infty$ ballooning and $n = 1$ kink ideal limits.

Successful steady-state tokamak operation requires operating at the highest possible beta while avoiding both ideal and resistive MHD instabilities which reduce confinement and induce disruption. Experimental results from a large number of tokamaks indicate that the high beta operational envelope of the tokamak is well defined by ideal magnetohydrodynamic (MHD) theory [1] and is given by $\beta(\%) \lesssim 4l_1 I/aB$ MA/m/T for a large range of conditions. The maximum beta values experimentally obtained, consistent with the ideal limit, are more than sufficient for the goals of long pulse burning experiments, such as ITER. The highest beta values achieved have historically been obtained in fairly short pulse discharges, often $<1-2$ sawteeth periods and $<1-2$ energy replacement times. In these discharges, the current profile is not fully relaxed. It is well recognized that the ideal limit depends on the details of the current density profile and pressure profile and it is expected that the bootstrap current from the pressure gradient at high beta can lead to lower MHD stability limits. Furthermore, in some previous experiments, the instabilities limiting the achievable beta are very clearly pressure driven resistive modes and significantly below the threshold predicted for ideal instabilities [2]. It is of interest to determine the maximum beta in discharges of sufficient length to have fully penetrated profiles and for opportunities for resistive modes to play a role.

The maximum operational beta in single-null divertor (SND), long-pulse discharges in DIII-D with a cross-sectional shape similar to the proposed ITER tokamak (Fig. 1) is found to be limited significantly below the threshold for ideal instabilities by the onset of resistive MHD instabilities. [A hard disruptive beta limit is usually considered to be due to ideal MHD instabilities, either the $n=1$ kink or the $n=\infty$ ballooning mode where n is the toroidal mode number.] The temporal evolution of a typical discharge is shown in Fig. 2; the beam power is increased gradually. There is a "soft" beta limit due to the onset of an $m/n = 3/2$ rotating tearing mode which saturates at an amplitude that decreases energy confinement by $\Delta\tau_E/\tau_E \approx -20\%$ [Fig. 2(b,c)] and a "hard" beta limit at slightly higher beta due to the onset of an $m/n = 2/1$ rotating tearing mode which grows to an amplitude that destroys the confinement and induces a disruption [Fig. 2(b,d)]. (Plasmas are neutral beam heated ELMing H-mode with sawteeth; the safety factor q_{95} is just above 3.)

Higher stable beta in these long-pulse discharges is successfully run by operating at either higher density \bar{n} and/or lower field and thus higher collisionality which suppresses both the $3/2$ and $2/1$ mode onsets. By long pulse, we mean that beta is evolving on a time scale long compared to the ELM and sawteeth periods and the energy replacement time τ_E . At fixed field, density \bar{n} is the control parameter varied

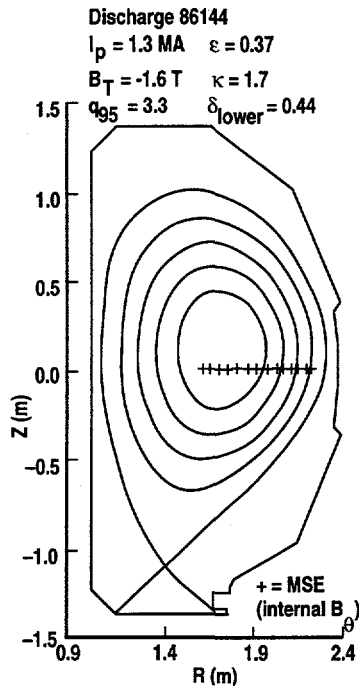


Fig. 1. Equilibrium cross section in DIII-D similar to that proposed for ITER. The 16 radial positions of the MSE diagnostic of poloidal field profile are also shown.

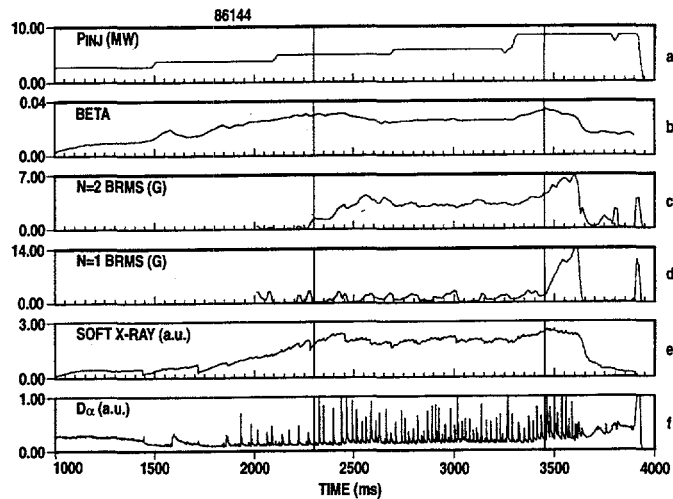


Fig. 2. Discharge #86144. (a) Injected beam power, (b) β from MHD reconstruction code EFIT, (c) rms amplitude of $n = 2$ rotating tearing mode ($m = 3, n = 2$), (d) rms amplitude of $n = 1$ rotating tearing mode ($m = 2, n = 1$), (e) central soft x-ray chord showing periodic sawteeth, and (f) D_α photodiode signal at divertor showing frequent edge localized modes. Note onset of $3/2$ mode at 2250 ms and $2/1$ mode at 3450 ms.

by gas puffing with the normalized beta $\beta_N \equiv \beta (\%) / [I_p / a B_T (\text{MA/mT})]$ and the normalized density $G \equiv \bar{n} (10^{14} \text{ cm}^{-3}) \pi a^2 / I_p$. The onset of the $2/1$ mode approaches the expected ideal limit of $\beta_N \approx 4 l_i \approx 3.8$ at $G \approx 1$ at high field (Fig. 3) where l_i is the internal inductance. As shown in Fig. 3, there is a $2/1$ tearing mode beta limit which increases with density and thus collisionality below which the plasma is stable. Successful quasi-steady-state operation without limiting modes at $\beta_N \approx 3$ was achieved with $G \approx 0.65$ as shown in Fig. 4 in comparison to a lower density discharge with reduced confinement due to an $n = 2$ tearing mode which further degrades at higher power due to an $n = 1$ tearing mode which leads to disruption. The ideal stability for the stable $\beta_N = 3$ discharge was analyzed by the code GATO. With $\beta_N = 3.2$ and $4 l_i = 3.6$, $n = \infty$ ballooning is stable on all surfaces, the $n = 1$ external kink is stable and the $n = 1$ internal kink is stable only if $q(0) > 1$.

Two possible means have been evaluated as the cause of the onset of these instabilities. Resistive tearing modes that occur at rational surfaces $q = m/n$ cause reconnection into islands of full width w . The island onset and growth can be due to either free energy from an unstable current J_ϕ profile ($\Delta' > 0$) or to a helical bootstrap current which amplifies a seed island ($\Delta' < 0$). These mechanisms are tested using accurate MHD equilibria reconstructions with the code EFIT [3] using the external magnetics, local measurements of the internal poloidal field with the 16 channel motional Stark effect diagnostic and the measured pressure profile.

Resistive MHD analysis of Δ' and stability is linearly computed from EFIT by analytical formulas [4,5] and by the PEST-III [6] and MARS [7] codes. Resistive non-

linear MHD analysis is computed on these equilibria with the PIES code [8]. Any changes to Δ' with beta and/or density may be due to current density profile modification by central beam-driven current and edge bootstrap and inductive currents.

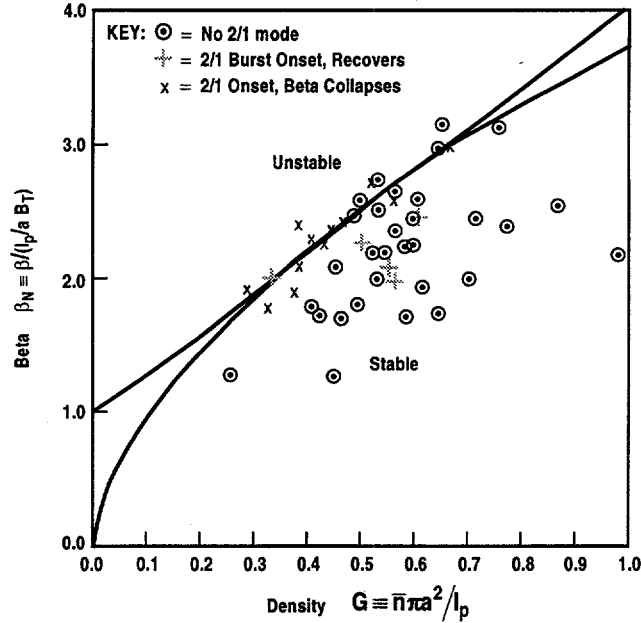


Fig. 3. $\beta_N \equiv \beta/(I_p/aB_T)$ versus $G \equiv \bar{n}\pi a^2/I_p$. X are onset of 2/1 mode, + are onset of a transient 2/1 mode from which the plasma recovers and O are discharges with no 2/1 mode. The curves are the 2/1 stability boundary determined by either a power law fit or to an offset linear fit. (The range of SND discharges is narrowed to $q_0 \approx 1$, $q_{95} < 4$ with $I_p \approx 1.3-1.6$ MA and $B_T = -1.3$ to -1.9 T.)

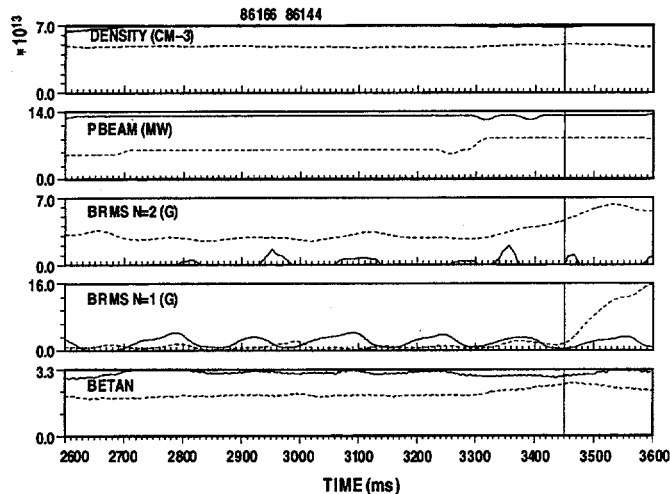


Fig. 4. Successful quasi-steady state operation without limiting modes at $\beta_N \approx 3$ is achieved (#86166, solid lines) by raising density/collisionality (as compared to #86144, dashed lines).

To explain the onset of both the 3/2 and 2/1 rotating resistive modes at higher beta and/or lower density (collisionality) would require steepening of the local grad J_ϕ at both $q = 3/2$ and $2/1$ in a plasma where the current profile is tightly constrained; sawteeth keep the axial $q \approx 1$ and the edge q_{95} is held fixed. Changes in grad J_ϕ are not clearly supported by the data. As an example, the reconstructions of matched discharges with similar beta ($\beta_N \approx 2.1$) but with different density and thus collisionality are shown in Fig. 5. The current density and q profiles are very similar. However, while both have a small saturated 3/2 mode, the lower density/collisionality discharge (#77968) is at the onset of the growth of a 2/1 mode which eventually collapses beta and produces a disruption. Conventional analysis does not clearly explain the difference in stability. The comparison of the $m/n=2/1$ unstable and stable discharge parameters of Fig. 5 and the linear and non-linear codes is given in Table I: note that $8 \bar{n}_{14}^3 R / \beta^2 (\%) B^4$ is an effective collisionality parameter. The high m and cylindrical linear approximations agree with each other as to the relative stability but neither agrees with the experimental stability. The PEST-III and MARS linear codes which do not use approximations also agree with each other but not with the experimental stability and the non-linear PIES code disagrees with the linear codes. There is a strong ∇p stabilization in the linear theory (sometimes called the "Glasser effect") that goes away when the pressure gradient is non-linearly flattened near the rational surface by the formation of a small but finite island.

A variety of cases are under calculation by all of the codes which include $\beta_N = 1.7-3.2$, $G = 0.3-1.0$ and with 3/2 onset, 3/2 saturated, 2/1 onset, 2/1 saturated and no 3/2 or 2/1 modes. Of the six different cases analyzed so far, the non-linear PIES code gets 3/2 islands in the five experimental cases which are unstable and no 3/2 islands in the stable case. PIES finds 2/1 islands in agreement with three of six experimental cases, in disagreement with two stable experimental cases, and no 2/1 island in agreement in one case which is experimentally stable. Sensitivity of both the linear and nonlinear code results to details of the current and q profiles makes comparison with experiment problematic.

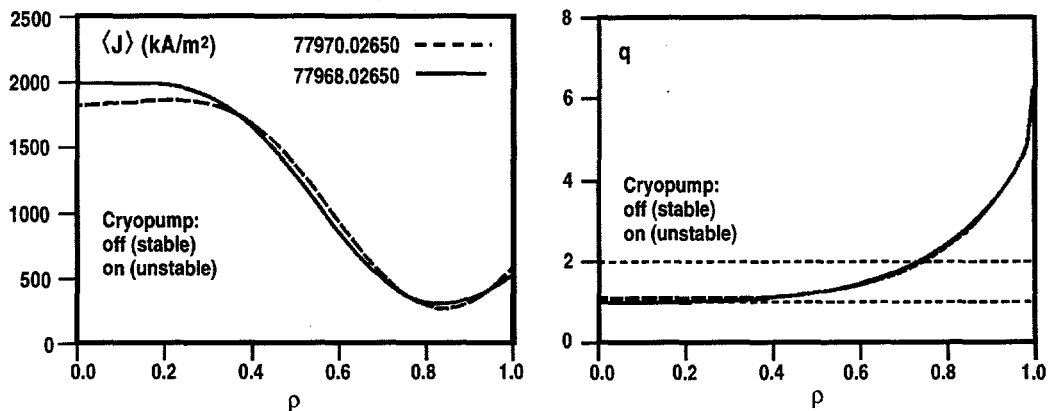


Fig. 5. Kinetic EFIT MHD reconstructions with internal poloidal field profile from MSE of a stable higher density discharge (77970.02650, dashed line) and an unstable cryopumped lower density discharge (77968.02650, solid lines). Measured internal pressure and B_θ profiles are used in the fits. At $t = 2650$ ms in the lower density higher temperature discharge, a 2/1 tearing mode begins to grow.

Table I. Comparison of m/n=2/1 Stability, Experiment, and Codes

| | | |
|---|------------------------------------|------------------------------------|
| | 77968.02650 | 77970.02650 |
| $\beta_N = \beta(\%) / (I_p/aB)$ | 2.0 | 2.3 |
| $G = \bar{n}^{14} \pi a^2 / I_p$ | 0.39 | 0.48 |
| $v_{\text{eff}} = 8 \bar{n}_{14}^3 R / \beta^2(\%) B^4$ | 0.018 | 0.027 |
| 2/1 ? (in experiment) | Onset, unstable | Stable |
| High m | Stable, $\Delta' r_g / 2m = -0.5$ | Stable, $\Delta' r_g / 2m = 0.0$ |
| Cylindrical | Unstable, $\Delta' r_g / 2m = 1.1$ | Unstable, $\Delta' r_g / 2m = 2.0$ |
| PEST-III | Stable | Stable |
| MARS | Stable | Stable |
| PIES | Unstable | Unstable |

An explanation of the experimental results can be made using the neoclassical bootstrap current destabilization of a seed island for $\Delta' < 0$, i.e. otherwise stable. This effect is increasingly more destabilizing with beta as the modified Rutherford equation for island growth is given by

$$\left(\frac{\mu_0}{1.22 \eta_{\text{nc}}} \right) \frac{dw}{dt} = \Delta' + \epsilon / 2 \beta_{\theta} \left(\frac{L_q}{L_p} \right) \left[\frac{w}{(w^2 + w_c^2)} \right] - \rho_{\theta i}^2 \beta_{\theta} g(\epsilon, v_i) \frac{(L_q/L_p)^2}{w^3}$$

where the second term on the RHS is usually ($L_q/L_p > 0$) destabilizing. Other MHD events such as sawteeth or ELMs often trigger the onset of the resistive modes, supporting the idea that they are neoclassically destabilized by a seed perturbation. The neoclassical destabilization of tearing modes requires the conditions to be right, i.e., high beta and low collisionality, and a seed island. The collisionality can enter (for $\Delta' < 0$) in either of two ways. In the " $\chi_{\perp}/\chi_{\parallel}$ " model [9], the pressure is not equilibrated on the perturbed flux surface when perpendicular transport χ_{\perp} across a seed island dominates over that along the island χ_{\parallel} , so that the critical island width w_c is an increasing function of collisionality. In the " ω^* " model [10], the toroidally enhanced ion polarization drift response of the plasma to the seed island due to inertial effects adds a stabilizing term to the modified Rutherford equation (the third term on the RHS) which dominates at small w . It has a collisional factor $g(\epsilon, v_i) = \epsilon^{3/2}$ for $v_i/\epsilon\omega_{*e} \ll 1$ and $g(\epsilon, v_i) = 1$ for $v_i/\epsilon\omega_{*e} \gg 1$ that can increase the critical island size a factor of 2-3 since our density scan causes $v_i/\epsilon\omega_{*e}$ to range from 0.05 to 4. (v_i/ϵ is the effective ion collision frequency and ω_{*e} is the electron drift frequency.)

The ITER-like discharges in DIII-D have both sawteeth and ELM perturbations with the sawteeth period 10 to 20 times that of the ELMs. Examination of the databases of the onset of m/n=3/2 and 2/1 modes shows: (1) in 14 of 17 cases of the onset of the 3/2 mode, the mode clearly starts on a sawtooth crash with 1 case on what may be an impurity burst, (2) in only 4 of 18 cases of the onset of the 2/1 mode does the mode start on a sawtooth crash and this may be coincident with an ELM or an ELM triggered by a sawtooth (as the ELMs are frequent, the causality with ELMs is not

definitive). Further evidence of neoclassical destabilization as seen in Fig. 2, (b) and (c), for the 3/2 mode is: (1) the initial growth is $|\tilde{B}_\theta| \sim \Delta t$ not Δt^2 ($dw/dt \sim w^{-1}$ not $dw/dt \sim \Delta'$), and (2) the saturated mode amplitude $|\tilde{B}_\theta| \sim \beta^2$ ($w \sim \beta$ not $w \sim \Delta'$).

If $\Delta' < 0$, the neoclassical stability depends on the size of the seed perturbation w relative to critical islands $w_c = (L_s/k\theta)^{1/2} (\chi_\perp/\chi_\parallel)^{1/4}$ and/or $w_g = [g(\epsilon, \nu_i) (L_q/L_p)/\epsilon^{1/2}]^{1/2} \rho_{\theta i}$. This is shown in Fig. 6 for the mode growth rate as a function of w for increasing β_θ . As beta is increased there is a critical beta and w for $dw/dt \geq 0$. If this beta is exceeded, a small island can grow to a large size [11]. The critical point is for $w_c^2 \gg w_g^2$, $\beta_\theta = -2 \Delta' w_c / [\epsilon^{1/2} (L_q/L_p)]$ and for $w_g^2 \gg w_c^2$, $\beta_\theta = -3 \Delta' w_g / 2 [\epsilon^{1/2} (L_q/L_p)]$. For typical DIII-D parameters, $w_c \approx 0.5$ cm and $w_g \approx 2$ cm compared to a ≈ 62 cm. As both w_c and w_g depend on beta, a self-consistent scaling is needed. For the $\chi_\perp/\chi_\parallel$ model taking $\chi_\parallel = \chi_{\text{BOHM}} (\rho_* v_*)^{-1}$ and $\chi_\perp = \chi_{\text{BOHM}} * \beta$, one gets critical $\beta \sim (-\Delta'a)^{4/3} (L_p/L_q)^{4/3} v_*^{1/3} \rho_*^{1/3}$ with $v_* \equiv [(m_e/m_i)^{1/2} v_{ei}/\epsilon] / \omega_{bi}$ and $\rho_* \equiv \rho_i/a$ dimensionless parameters. For the ω_* model, $\beta_{\text{crit}} \sim -\Delta'a (L_p/L_q) g(\epsilon, \nu_i)^{1/2} \rho_*$ yielding a different dependence upon collisionality and gyroradius. Of course, if Δ' or profiles vary with beta and/or collisionality, the scaling would be yet different.

As the neoclassical destabilization with beta depends on collisionality in different ways, empirical fits of critical beta for onset of 3/2 or 2/1 tearing were made to v_* , ρ_* , etc. for as wide a range of variables as possible. The database of discharges at the onset of 3/2 tearing or 2/1 tearing scans $B_T = 0.9-2.1$ T at $I_p = 0.65-1.5$ MA with $q_{95} < 4$, $\bar{n}_{14} = 0.26-0.82$, with critical $\beta = 1.73-5.16\%$. The radial scale lengths at $q=m/n$ for q , T_e , and T_i at the 3/2 and 2/1 mode onsets, respectively, do not vary significantly. [The H-mode core density profile is fairly flat in all cases.] For the 3/2 mode onset, the mean $L_q/a = 0.55 \pm 0.05$, $L_{T_e}/a = -0.39 \pm 0.06$, and $L_{T_i}/a = -0.33 \pm 0.03$. The mean Δ' using the high m approximation is $-9.4 \pm 1.5 \text{ m}^{-1}$. For the 2/1 mode onset, the mean $L_q/a = 0.40 \pm 0.03$, $L_{T_e}/a = -0.41 \pm 0.08$, and $L_{T_i}/a = -0.38 \pm 0.10$. The mean Δ' using the high m approximation is $-8.0 \pm 1.8 \text{ m}^{-1}$. Thus the principal experimental variables for the tearing mode destabilization are beta, collisionality, and to a much lesser extent gyroradius. A fit to $\beta_{\text{crit}} \sim v_*^x \rho_*^y$ was done

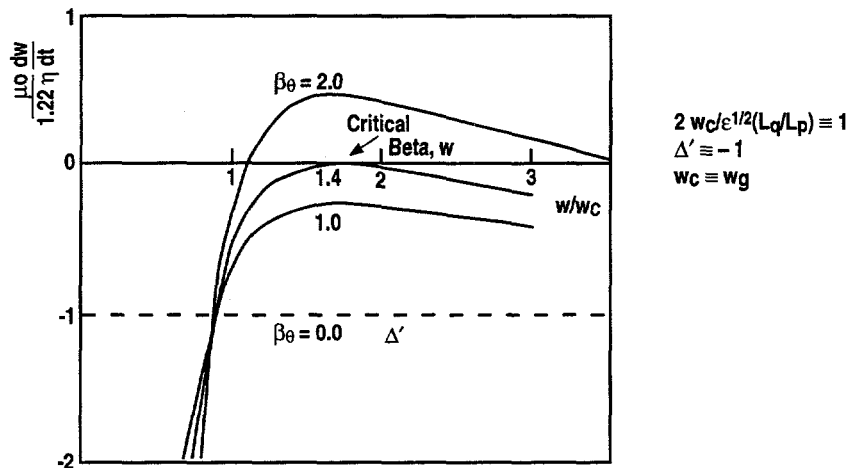


Fig. 6. Neoclassical model for island growth rate versus island size w for $\Delta' < 0$ and increasing values of beta. The critical beta, w for $w \geq 0$ is indicated.

in two ways. For global parameters, one expects for $T_e = T_i \sim \beta B^2 / \bar{n}$, $v_* \sim \bar{n}^3 R / B^4 \beta^2$, $\rho_* \sim \beta^{1/2} / \bar{n}^{1/2} a$ and $a \sim R$ at fixed q_{95} so that

$$\beta \sim v_*^x \rho_*^y \sim \bar{n}^{1+2x-y/2} R^{1+2x-y/2} / B^{1+2x-y/2} \cdot \frac{4x}{B^{1+2x-y/2}}$$

This global scaling allows a survey of the gross parameters under direct control of the physics operator. For the onset of the 3/2 mode, the best fit gives $x = 0.42$ with no significance to y . The result (\odot) is shown in Fig. 7(a) with the expected ideal limit (\times) of $4 I_i / aB$ for comparison and the expected ITER limit ($\bar{n}_{14} = 1.3$, $R = 8.0$ m, $a = 2.8$ m, $B = 5.7$ T, $I = 21$ MA) if $G = 1.5$ can be achieved. The soft 3/2 tearing limit is as much as a factor of 2 below the ideal limit. For the onset of the 2/1 mode, the best fit gives $x = 0.47$ with again no significance to y . The results are shown in Fig 7(b). At high density, low field, the 2/1 tearing occurs at a beta near the expected ideal limit. The dependence on the local parameters of the soft 3/2 tearing mode beta limit was also fitted and is shown in Fig. 8(a). For the 3/2 mode, the range in v_* is only 3.1 and in ρ_* only 1.4 as at low B, the 2/1 mode turns on first and the discharges disrupt. The dependence on the local parameters of the hard 2/1 tearing mode beta limit was also fitted and is shown in Fig. 8(b). v_* varies a factor of 16 while ρ_* varies a factor of 1.6. The ρ_* dependence may be anything from 0 ~ 1/3 within the uncertainty. A fit using $v_i / \epsilon \omega_{*e}$ (which is more relevant for the ω^* model) instead of v_* was almost as good.

As the higher field, larger ITER device is expected to have both lower v_* and ρ_* , extrapolation to ITER requires knowing what Δ' really is or will be, understanding of which of the neoclassical threshold mechanisms dominates, how β_{crit} scales with v_* (and ρ_*), and how the necessary seed perturbation island (particularly from sawteeth and ELMs) for the neoclassical destabilization scales. An interesting possibility is whether a higher stable beta can be obtained by operating at $q > 1$ to eliminate sawteeth perturbations or with negative magnetic shear which is neoclassically stabilizing for modes inside the negative shear reversal region ($L_q / L_p < 0$).

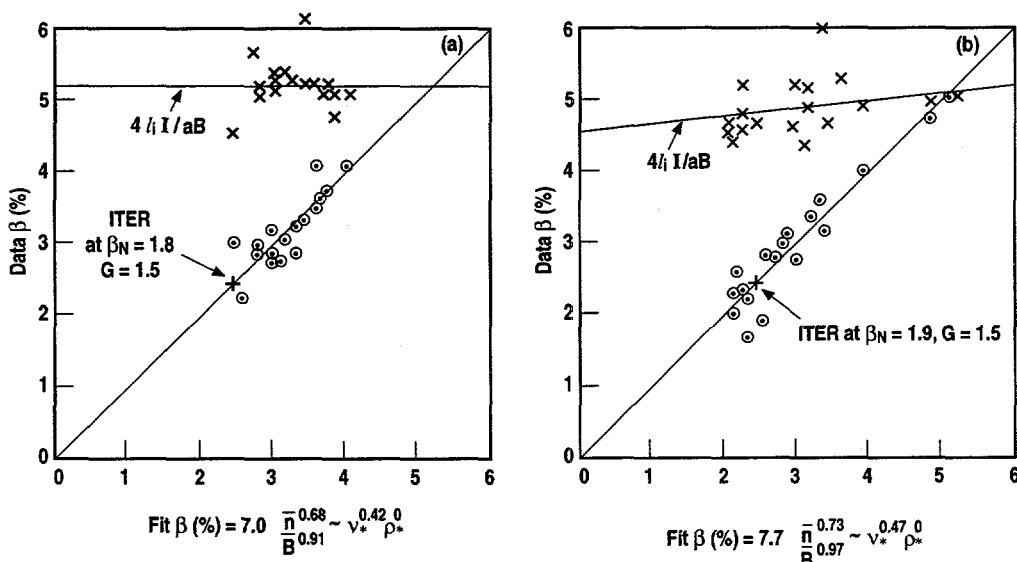


Fig. 7. (a) Onset of 3/2 tearing (\odot) in DIII-D fitted to global parameter combinations. (b) Onset of 2/1 tearing (\odot) in DIII-D fitted to global parameter combinations. Expected ITER beta limit is also shown ($+$) as well as expected ideal limit. (\times).

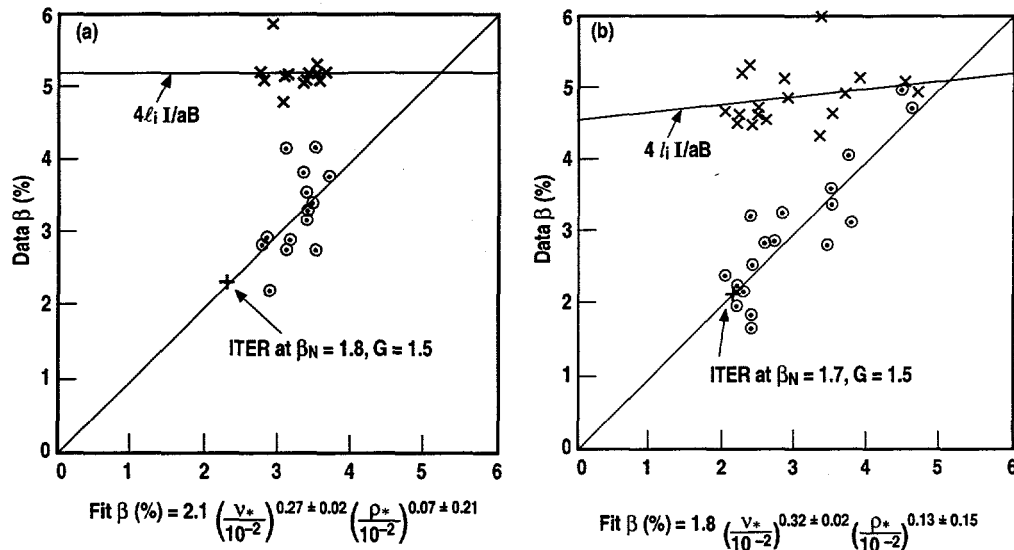


Fig. 8. (a) Onset of 3/2 tearing (\odot) in DIII-D fitted to local parameters. (b) Onset of 2/1 tearing (\odot) in DIII-D fitted to local parameters. Expected ITER beta limit is also shown (+) as well as expected ideal limit (\times).

ACKNOWLEDGMENTS

Work supported by the U.S. Department of Energy under Contract Nos. DE-AC03-89ER51114, DE-AC02-76CH03073, Grant No. DE-FG02-92ER54139, and in part by the Swiss National Science Foundation and the U.K. Department of Trade and Industry and EURATOM. Cylindrical delta prime calculations by Frank Waelbroeck of the IFS are appreciated.

REFERENCES

- [1] STRAIT, E.J., et al., Phys. Plasmas **1** (1994) 1415.
- [2] STRAIT, E.J., et al., Phys. Rev. Lett. **62** (1989) 1282.
- [3] LAO, L.L., et al., Nucl. Fusion **25** (1985) 1611.
- [4] HEGNA, C.C. and CALLEN, J.D., Phys. Plasmas (1994) 2308.
- [5] FURTH, H.P., et al., Phys. Fluids **16** (1973) 1054.
- [6] PLETZER, A., et al., J. Comput. Phys. **115** (1994) 530.
- [7] BONDESON, A., et al., Phys. Fluids B **4** (1992) 1889.
- [8] REIMAN, A.H., and GREENSIDE, H.S., J. Comput. Phys. **87** (1990) 349.
- [9] FITZPATRICK, R., Phys. Plasmas **2** (1995) 825.
- [10] WILSON, H.R., et al., Phys. Plasmas **3** (1995) 248.
- [11] CHANG, Z., et al., Phys. Rev. Lett. **74** (1995) 4663.